Nanoscale

PAPER

View Article Online
View Journal | View Issue

Cite this: *Nanoscale*, 2019, **11**, 17869

Tracking the DNA complexation state of pBAE polyplexes in cells with super resolution microscopy†

Roger Riera,[a,b] Natalia Feiner-Gracia,[a] Cristina Fornaguera,[b] Anna Cascante,[b,c] Salvador Borrós[b,c] and Lorenzo Albertazzi *[a,d]

Received 3rd April 2019,
Accepted 11th September 2019

DOI: 10.1039/c9nr02858g

rsc.li/nanoscale

The future of gene therapy relies on the development of efficient and safe delivery vectors. Poly(β-amino ester)s are promising cationic polymers capable of condensing oligonucleotides into nanoparticles – polyplexes – and deliver them into the cell nucleus, where the gene material would be expressed. The complexation state during the crossing of biological barriers is crucial: polymers should tightly complex DNA before internalization and then release to allow free DNA to reach the nucleus. However, measuring the complexation state in cells is challenging due to the nanometric size of polyplexes and the difficulties to study the two components (polymer and DNA) independently. Here we propose a method to visualize and quantify the two components of a polyplex inside cells, with nanometre scale resolution, using two-colour direct stochastic reconstruction super-resolution microscopy (*d*STORM). With our approach, we tracked the complexation state of pBAE polyplexes from cell binding to DNA release and nuclear entry revealing time evolution and the final fate of DNA and pBAE polymers in mammalian cells.

Introduction

Gene therapy has been growing in the last few years as a promising tool to treat diverse acquired and genetic diseases using nucleic acids as therapeutics. Several applications are currently explored at the preclinical and clinical stage in the fields of cancer, monogenic or infectious diseases.[1] The main challenge of gene therapy is to deliver the intact oligonucleotide cargo into the specific site of action, *i.e.* the cytoplasm for RNA and the nucleus for DNA, overcoming a series of cellular barriers. First, gene carriers have to maintain their structure stable through the systemic circulation and the extracellular environment. Then, they must bind to the cell membrane and be taken up by the cell. Lastly, they need to evade lysosomal degradation and recycling, to release their cargo intact at the end. For DNA-based therapeutics, there is an additional barrier to overcome as the nucleic acid has to reach the nucleus crossing the nuclear membrane. Viruses have naturally evolved to specifically surpass these barriers; for this reason, they have been widely used in gene therapy. Indeed, most of the clinical gene delivery systems approved to date (Gendicine[2] and Oncorine[3] in China, Glybera[4] in EU and Luxturna[5] in the USA) are based on viral vectors. However, safety concerns, high production cost and low loading capacity have triggered the development of non-viral gene delivery systems. These systems are based on synthetic materials that combine with DNA/RNA into nanostructures and serve as a carrier to protect and direct the therapeutic cargo. A wide variety of synthetic gene delivery systems have been tested so far. Typical approaches include lipid vesicles (*e.g.* DOTAP,[6] DOPE,[7] and DC-Chol[8]), polyplexes (*e.g.* poly(ethyleneimine)[9] and poly(lysine)[10]) and inorganic carriers (*e.g.* gold nanoparticles).[11–13] Recently, ONPATTRO® has been approved by the FDA and EMA as the first lipid-based gene delivery system for the treatment of polyneuropathy of hereditary transthyretin-mediated (hATTR) amyloidosis in adults.[14]

From the variety of non-viral carriers, polyplexes have been widely studied as potential gene delivery carriers. They are nano-sized complexes formed through the electrostatic interaction of cationic polymers and nucleic acids. Their low toxicity profile, facile chemistry and promising transfection efficiency have drawn a lot of attention.[15] However, it is important to underline that the design of highly efficient polyplexes that are able to successfully overcome all the biological bar-

[a]*Nanoscopy for Nanomedicine, Institute for Bioengineering of Catalonia, Barcelona, Spain. E-mail: l.albertazzi@tue.nl*
[b]*Grup d'Enginyeria de Materials (GEMAT), Institut Químic de Sarrià, Universitat Ramon Llull, Barcelona, Spain*
[c]*Sagetis-Biotech, Barcelona, Catalonia, 08017, Spain*
[d]*Department of Biomedical Engineering, Institute for Complex Molecular Systems (ICMS), Eindhoven University of Technology, Eindhoven, Netherlands*
†Electronic supplementary information (ESI) available. See DOI: 10.1039/c9nr02858g

riers is still a major challenge in gene delivery. For this reason, more detailed knowledge about the polyplex structures and interactions with cells are crucial for the development of next generation non-viral gene delivery carriers. This is not a trivial issue as the nanometric size, multicomponent nature and dynamic behaviour (*e.g.* assembly–disassembly) of polyplexes pose a serious challenge to their study.

Here we propose a 2-colour super-resolution microscopy-based method to study polyplex stability and DNA release inside cells. Super-resolution techniques are able to break the light diffraction limit of conventional fluorescence microscopy, restricted to 200–300 nm.[16] Polyplexes are typically 50–200 nm in size, therefore, 2-colour super resolution microscopy can resolve their 2-component structure and their close interaction with biological components. Super-resolution microscopy, initially developed to study biological structures, has recently proved to be a powerful tool to study nanoparticles *in vitro* and in cells.[17–19] Recently, we have proven the applicability of 2-colour super-resolution microscopy for polyplex stoichiometry quantification.[20]

In our approach, direct stochastic optical reconstruction microscopy (*d*STORM)[21,22] is used to obtain high-resolution images of polyplexes where their structure is clearly resolved. Previously used electron microscopy techniques to resolve polyplex structures could not discriminate between the oligonucleotide cargo and polymer as it can be done using two-colour fluorescence microscopy imaging. Moreover, STORM is part of the single-molecule localization microscopy (SMLM) techniques,[23] which allow precise identification and quantification of both polyplex components independently at the single-molecule level.

In the present work, we applied 2-colour *d*STORM to track oligopeptide end-modified poly(β-amino ester) (pBAE) polyplexes carrying plasmid DNA (pDNA) in cultured cells. pBAE polyplexes have proven to be promising gene delivery carriers because of their high transfection efficiency combined with low toxicity and increased biodegradability.[24,25] Moreover, their structure allows for further functionalization both at the termini and at lateral chains to facilitate nucleic acid complexation and to modulate and enhance their transfection efficiency in a cell-type selective way.[26,27] pBAEs have been used for a wide variety of targets, such as *in situ* programming of T-cells,[28] enhanced angiogenesis in stem cells[29] and cancer treatment.[30,31] Recently, we have developed a new family of oligopeptide terminated poly(β-amino ester)s that are able to form polyplexes with different kinds of oligonucleotides and are able to efficiently transfect them both *in vitro* and *in vivo*.[26,32–35] With a combination of *d*STORM microscopy and single molecule image analysis tools, we were able to quantify their stability and DNA release during cell uptake, trafficking and nuclear entry, *i.e.* the main barriers towards successful transfection. Our data allow for a better understanding of how polyplexes behave inside cells and help in their re-design to control DNA release.

Results and discussion

Poly(β-amino ester) polymers were synthesized by mixing 1,4-butanediol diacrylate and hexylamine in a 1 : 1 ratio as described in the Materials and methods section. The end-acrylated molecules were later functionalized with tri-arginine oligopeptide moieties at both ends (C6-CR3). The oligopeptide modification was carried out using a thiol reaction with cysteine-ended oligopeptides. The transfection efficiency of C6-CR3 has been described in previous studies.[34] The polyplex cargo consisted of a plasmid DNA (3.5 kb) containing the GFP gene that serves as a reporter of transfection. Polyplexes were prepared by mixing pBAE and pDNA in a 25 : 1 mass ratio and lyophilized in small aliquots. For imaging purposes, as shown in Fig. 1, pBAE and pDNA were labelled with a pair of dyes suitable for *d*STORM. pBAE was functionalized with Cy5 in an average 1 : 1 dye : polymer ratio and pDNA with Cy3 in an average 10 : 1 dye-plasmid ratio as described in the Materials and methods section.

For *d*STORM imaging, labelling density needs to be adjusted to obtain an optimal dye blinking rate. In order to

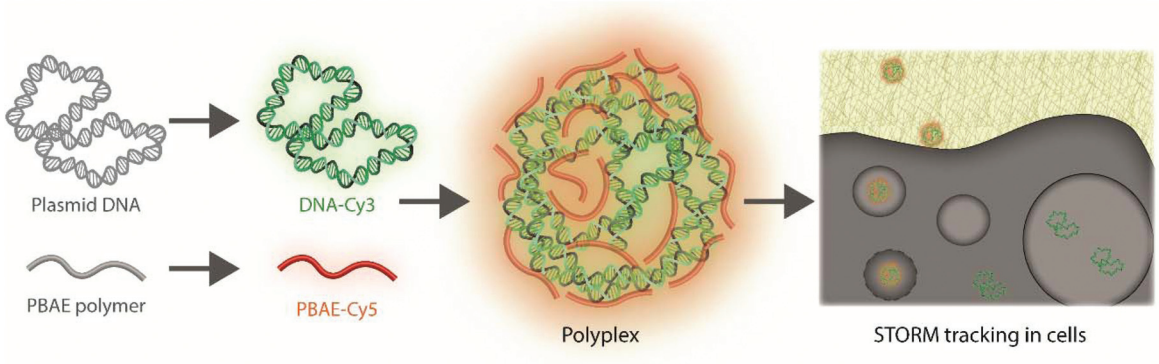

Fig. 1 Workflow of polyplex formulation and *d*STORM imaging. Firstly, the pBAE polymer and pDNA are labelled with Cy5 and Cy3, respectively. Polyplexes are formulated by nanocomplexation, mixing the two components, and incubating with COS7 cells afterwards to perform transfection. Lastly, the polyplex complexation state is tracked by *d*STORM imaging.

identify individual molecules, only one dye has to be emitted in a diffraction-limited area per frame. However, to completely reconstruct the image, it is desired to collect as much localizations as possible before the dye bleaches irreversibly. Therefore, we optimized the labelling density (*i.e.* the ratio between labelled and unlabelled molecules) for pBAE and pDNA to 1% and 25% labelled molecules, respectively.

Polyplexes were prepared by the electrostatic interaction between the PBAEs and the DNA, and lyophilized to prolong their storage stability. Furthermore, they were characterized by DLS to measure its hydrodynamic size before and after lyophilization. The hydrodynamic diameter of polyplexes suffered a non-significant increase after lyophilisation (Table S1†), although, they were still disperse in discrete nanostructures, as expected from previous results.[33] Labelled polyplexes were then used for cellular imaging as schematically shown in Fig. 1.

First, we imaged polyplexes adsorbed on a glass slide – before cell administration – in order to show the ability of *d*STORM to visualize the two components with sub-diffraction resolution and, therefore, resolve individual polyplexes. Fig. 2 shows the diffraction-limited images of each component (2a and 2b) and the *d*STORM reconstructed image of both (2c). Because our pBAE polyplexes have a size below the diffraction limit of 200–300 nm (Table S1†), their structure is not well resolved with conventional fluorescence techniques (the polyplex appears as a blurred spot); however, it is clearly resolved with *d*STORM. The narrower and non-stepwise intensity profile of the *d*STORM image (Fig. 2d) corroborates the better visualization of the polyplex structure. Although polyplexes can be resolved by electron microscopy (Fig. S1†), *d*STORM allows the visualization of the distribution of the polymer and pDNA independently, thanks to its multicolour ability. *d*STORM images show that pDNA is concentrated in an inner area of the polyplex, while pBAE is found in the core and forming a shell around it. This suggests that the pDNA interacts with the polymer to condense into concrete mixed structures, but there is also an additional external polymer layer.

*d*STORM imaging not only allows precise resolving of the composition of polyplexes, but also gives quantitative information at the single molecule level. We were able to observe a high amount of free pBAE molecules in solution together with polyplexes (Fig. 2c). Notably, this is not detectable with commonly used techniques to characterize polyplexes, such as DLS or NTA, and neither conventional fluorescence microscopy is sensitive enough to detect single molecules.[36] Although it is the first time that the free polymer is directly observed, it was previously hypothesized by the presence of small polymer aggregates in TEM images (Fig. S1†). The effect of the free cationic polymer is poorly studied, despite its possibility of having a great impact on polyplex formation and delivery performance. Surprisingly, although not being part of a polyplex, these free pBAE molecules are needed to form stable polyplexes. Previous studies demonstrated lower polyplex stability when the polymer concentration was reduced in the formulation.[37] This is attributed to a dynamic equilibrium established between the polymer in the polyplex and the free polymer to maintain the encapsulated gene material (Fig. S2†). In studies using similar systems, we tried to clean excess polymer from the samples, and although polyplexes seem to maintain their size (Table S1†), they lose their capacity to transfect (Fig. S3†). Moreover, recent studies showed that the addition of the free polymer with endosomal escape capabilities to polyplexes without this property increased the polyplex transfection efficiency, suggesting that these free molecules have a great influence on this crucial step for gene delivery.[38] Therefore, STORM is an ideal technique to study both the polyplexes and the free polymers at the same time.

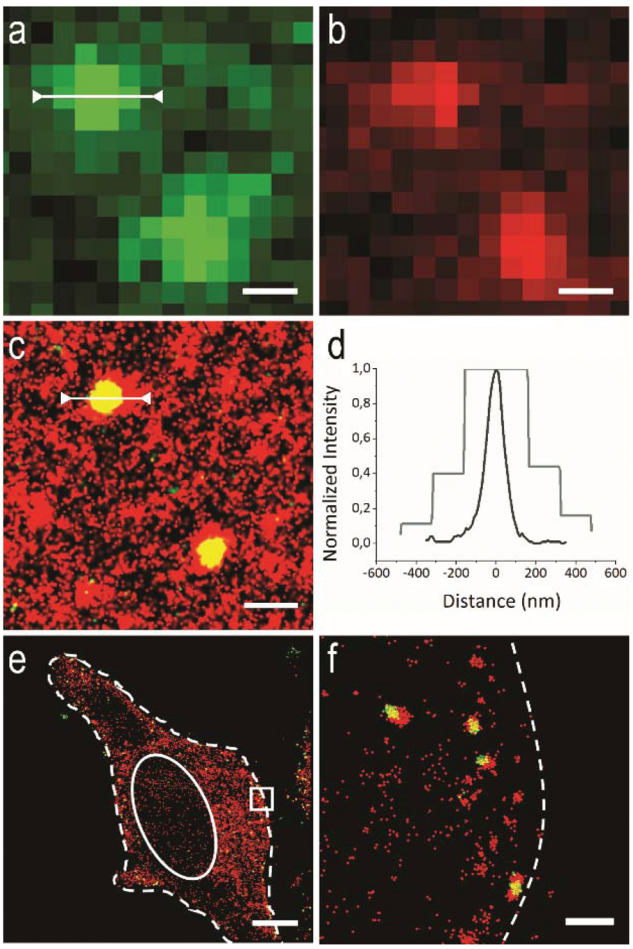

Fig. 2 *d*STORM images resolve the pBAE polyplex structure on a glass slide and in cells. (a–c) Images of polyplexes on a glass slide (scale bar = 500 nm). (a) and (b) show the conventional fluorescence images of pDNA and the pBAE polymer, respectively. Image c shows the reconstructed *d*STORM image of both components. (d) Intensity profile of a polyplex (white lines on images a and c) with low resolution (grey) and *d*STORM (black) images. (e) *d*STORM image of pBAE polyplexes incubated for 30 minutes on COS7 cells (scale bar = 10 μm). (f) Augmented view of polyplexes on the white square of image e (scale bar = 1 μm).

In order to study how pBAE polyplexes behave inside cells, we incubated COS-7 cells with polyplexes followed by fixation and imaging. Firstly, we successfully obtained 2-colour

*d*STORM images of polyplexes inside cells, as shown in Fig. 2e and f. Interestingly, non-complexed polymers and polyplexes were both being internalized by the cell. After 30 minutes of incubation, we could distinguish a different internalization kinetics of polyplexes and free polymers. Polyplexes were only found close to the cell membrane (Fig. 2e and f), meanwhile free polymers were widely distributed inside the cell. This observation gives insight into the mechanism of internalization of both components. Cationic polymers like pBAEs are known to produce nanoscale defects in cell membranes, which is the major cause of their cytotoxicity. Previous studies showed that even non-cytotoxic concentrations of these polymers produced such defects, leading to a leak or internalization of small molecules and proteins.[39] Therefore, as the free

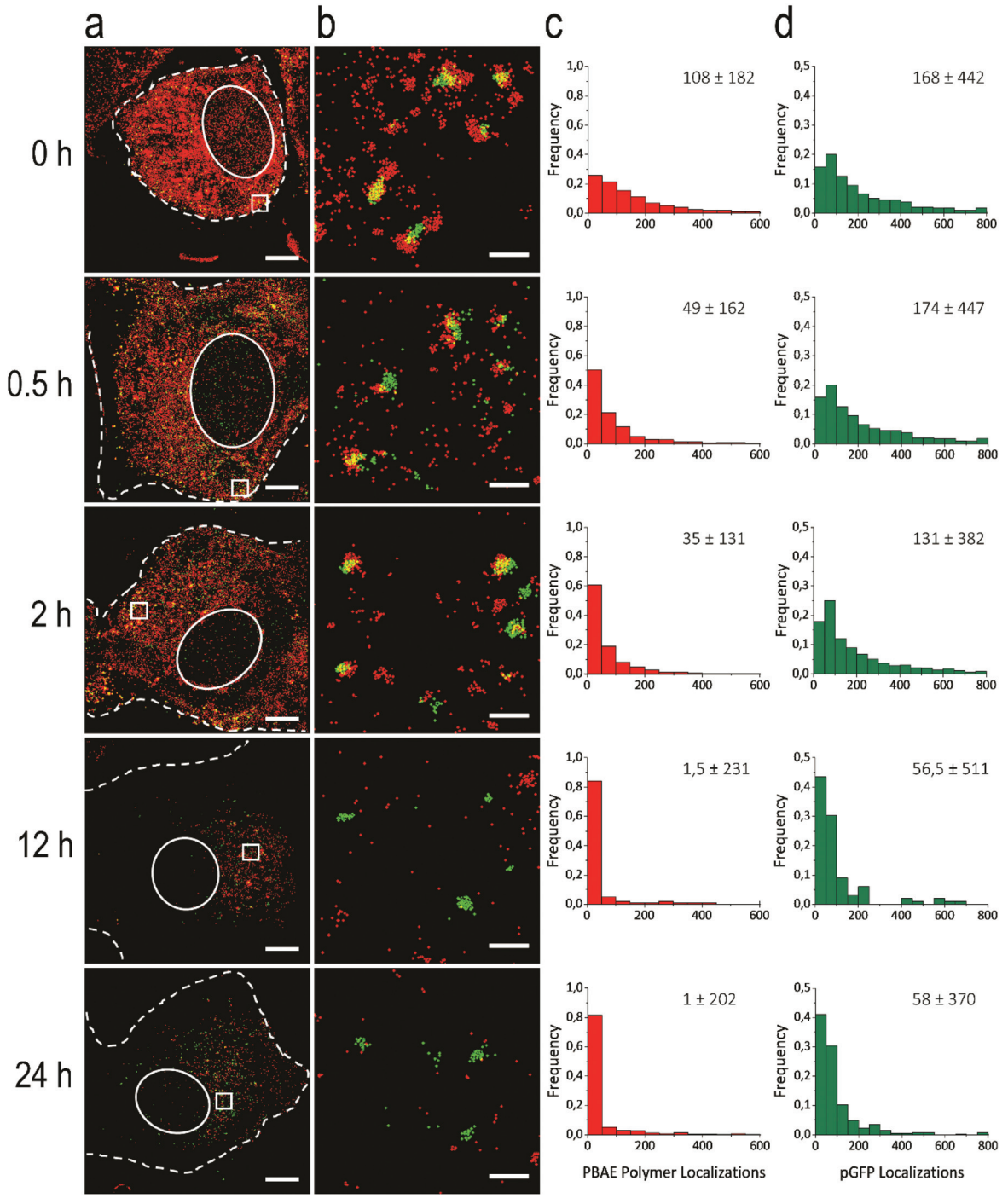

Fig. 3 *d*STORM image quantification shows how pBAE polyplexes decomplexate over time inside the cell. (a) *d*STORM images of polyplexes internalized by COS-7 cells (scale bar = 10 μm). (b) Enlarged view of polyplexes on the white square (scale bar = 500 nm). (c) Quantification of pBAE polymer localizations in each polyplex (median ± SD). (d) Quantification of pDNA localizations in each polyplex (median ± SD).

polymer has a faster uptake kinetics and it disperses into the cytoplasm, it probably enters the cell through membrane irregularities rather than by endocytosis, as polyplexes do.[40]

To further understand polyplex trafficking, we performed a pulse-chase experiment: COS-7 cells were incubated with polyplexes for 30 minutes and grown in fresh media before fixation at different time points. Representative *d*STORM images of cells show the localization of polyplexes at the different time points (Fig. 3a and b). First, we observe polyplexes close to the cell membrane (t_0), just after internalization. During the initial hours ($t_{0.5-2}$), polyplexes look more dispersed inside the cell and are not only restricted to the cell membrane. After internalization, polyplexes are known to be trafficked through the endolysosomal pathway with different possible fates, such as lysosomes, Golgi or recycled vesicles.[41,42] Lastly, we observe polyplexes mostly in the perinuclear region (t_{12-24}), the fate of the non-recycled polyplexes. This localization has been proposed to be the previous step to nuclear entry.[43,44]

Thanks to the 2-colour labelling, these *d*STORM images also provide useful information about the polyplex composition in time. Initially, we observed complexed structures that contain both, polymers and pDNA (t_{0-2}), as seen in the *d*STORM images of polyplexes outside cells (Fig. 2c). However, at later time points, we could only observe discrete pDNA not covered by the polymer (t_{12-24}), making it evident that the pDNA release has occurred after a few hours of internalization. Moreover, we observed a reduction in the amount of the free polymer that, as mentioned previously, enters rapidly in the cell. In the initial hours (t_{0-2}), there is an abundant and diffuse free polymer inside the cells, which is lost afterwards. Our pBAE polymer contains ester bonds in its structure, so polymer chains can be degraded and removed from the cell. It is important that the polymer is removed quickly from the cell to reduce cytotoxicity. This is the first measurement of intracellular disassembly and pDNA release from polyplexes, a key step towards efficient transfection. It shows the potential of *d*STORM to complement the existing techniques for the study of polyplexes and support the rational design of improved gene carriers.

To further corroborate our results, we designed a quantitative analysis for the single molecule localization microscopy (SMLM) data obtained using *d*STORM. Briefly, a MATLAB script is used to identify single polyplexes by clustering pDNA localizations and quantifying the number of pBAE localizations in each cluster. A minimum of 200 polyplexes were analysed in each time point. To represent the high heterogeneity of our samples – note the high values in standard deviation – we plotted the resulting data in histograms (Fig. 3c and d). We observed an initial decay in the amount of polymer, from 108 to 49 localizations per polyplex in the first 0.5 h, while pDNA remained constant. This could have been caused by the initial interaction of the external polymer layer with the cell membrane during internalization, while, the pDNA packing has not been affected yet. Later, we observed a substantial decrease of polymer dropping to 1.5 localizations per polyplex at 12 h. We also observed a decrease in the number of pDNA localizations,

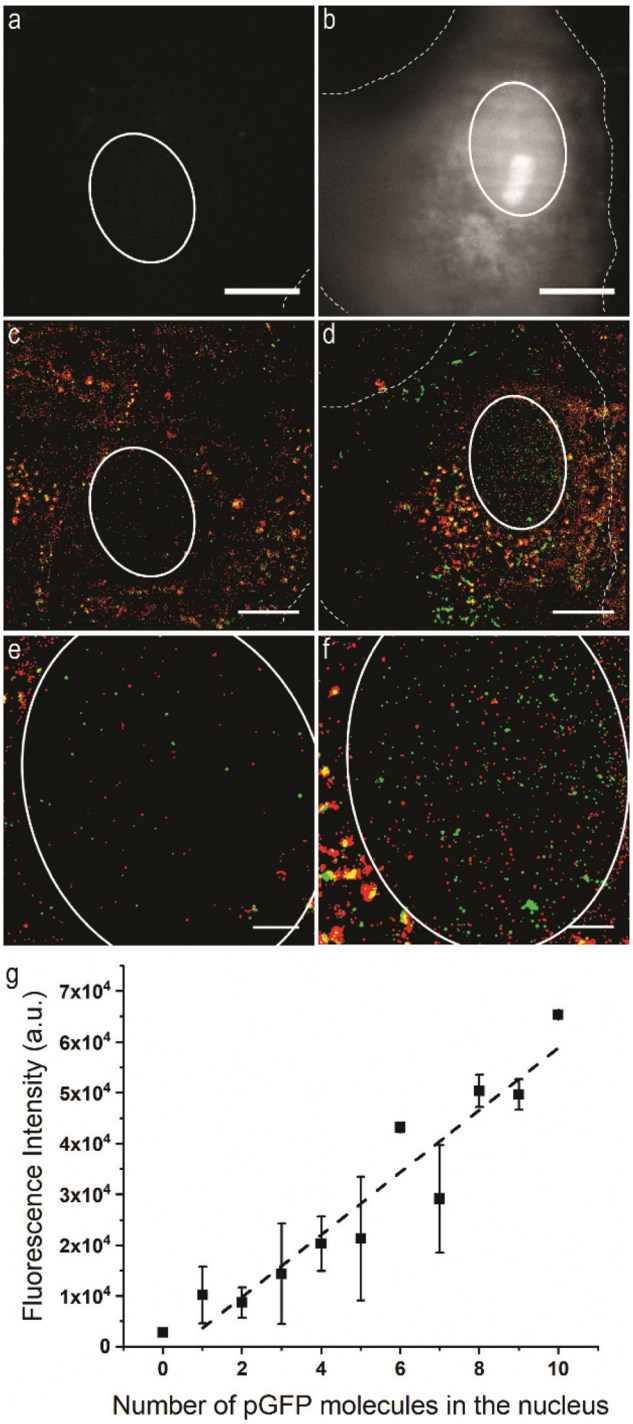

Fig. 4 GFP fluorescence correlation with nuclear pDNA molecules. (a–c) Images of a low GFP expressing cell. GFP fluorescence image (a, scale bar = 10 μm) shows a low number of pDNA molecules inside the nucleus in the *d*STORM images (b, scale bar = 10 μm; c, scale bar = 5 μm). (d–f) Images of a high GFP expressing cell. GFP fluorescence image (d, scale bar 10 μm) shows a high number of pDNA molecules inside the nucleus in the *d*STORM images (e, scale bar = 10 μm; f, scale bar = 5 μm). (g) The graph shows the correlation between the GFP fluorescence intensity (mean ± SD) and the number of pDNA molecules in the nucleus of 46 cells. The linear regression has an R^2 value of 0.9.

which remained constant up to 48 h (Fig. S4†). At this point, we were no longer detecting polyplexes, but single pDNA molecules, corroborating that DNA release was complete. Overall, we demonstrate that our pBAE polyplexes decomplex within 12 h; free pDNA molecules are released in the perinuclear region and the remaining polymer is recycled out of the cell. The ability to track decomplexation in space and time makes *d*STORM a useful tool to evaluate polyplex stability and release ability.

The last crucial step in the delivery process is nuclear entry. To follow it, we designed an experiment to visualize GFP-coding pDNA molecules inside the nucleus and related it with the transfection efficiency of the polyplexes. For this particular experiment, polyplexes were prepared with all pDNA molecules labelled, as we were interested to localize every single DNA plasmid. Briefly, we incubated COS7 cells with polyplexes for 48 h, a standard incubation time for transfection experiments.[26] We acquired a *d*STORM image of the polyplexes together with an epifluorescence image of GFP expression to assess the transfection efficiency of each cell. We observed a broad distribution in the transfection efficiency and the presence of pDNA in the nucleus among cells, although all the cells had a significant amount of polyplexes internalized (Fig. 4a–f). Therefore, we decided to determine whether there was a correlation between the GFP expression and the amount of pDNA in the nucleus. pDNA localizations were clustered with a custom Matlab script to quantify the number of pDNA molecules in the nucleus and then it was correlated with the fluorescence intensity of GFP epifluorescence images (Fig. 4g). We concluded that despite having some variability, there is a high correlation coefficient (R^2 = 0.9) between both the parameters. These observations demonstrate that the variability in transfection among cells arises mainly from a differential nuclear entry. Interestingly, although most of the cells have a high amount of polyplex in the cell, it did not result in a successful nuclear entry for all of them. This fact could be as a result of poor nuclear targeting/retention (absence of an NLS sequence), inability to escape from endosomes, or that the trafficking route, although bringing pDNA to the perinuclear area, is not promoting it to enter into the nucleus. Also, cell division is known to play a key role in nuclear entry, therefore, heterogeneity may be produced by cells that divided after pDNA release and cells that did not. Moreover, we observed that plasmid molecules found in the nucleus are not complexed with the polymer. This consistently agrees with our previous results that single pDNA molecules are released into the perinuclear area before nuclear entry.

Conclusions

Our study brings key information on pBAE polyplex delivery using 2-color *d*STORM. The independent labelling of pBAE and pDNA allows the determination of the polyplex composition along the whole delivery process. We provided qualitative and quantitative results to determine the kinetics of polyplex decomposition and the time frame of DNA release inside cells. With our single particle analysis, we could also assess the heterogeneity within polyplexes to reveal the complexity of our sample. Moreover, the single molecule sensitivity of our method showed the presence of abundant free pBAE molecules that were also internalized inside the cell. Finally, nuclear entry experiments revealed that pDNA molecules were entering the nucleus already exposed and that the presence of these pDNA molecules in the nucleus correlate with the expression of the encoded GFP. The work presented here is the first application of quantitative super resolution microscopy to study polyplex decomplexation and DNA release, to our knowledge. We revealed the key parameters in the delivery process of polyplexes that multicolour super resolution microscopy can assess to better understand and design them.

Materials and methods

Reagents

Paraformaldehyde (PFA), glucose oxidase from *Aspergillus niger*, cysteamine (MEA), catalase from bovine liver, glucose, sucrose, AcONa, HEPES and PBS were purchased from Sigma-Aldrich®. Fetal Bovine Serum (FBS), Dulbecco's Modified Eagle's Medium (DMEM), glutamine, penicillin and streptomycin were purchased from Gibco®. Plasmid pMAX-GFP (3486 bp) was produced and purified from *E. coli* and labelled with the Cy3 Label IT® Tracker™ Intracellular Nucleic Acid Localization Kit from Mirus, following the supplier's protocol. Labelling density was adjusted to 10 dye molecules per plasmid DNA (pDNA). This was determined from the ratio of Cy3 and DNA concentrations measured using a NanoDrop ND-1000 (Thermo Fisher, Massachusetts, USA).

The arginine end-modified poly(β-amino ester) polymer was synthesized following a two-step procedure described in the literature. In brief, first, an acrylate-terminated polymer, C6 polymer,[34] was synthesized by an addition reaction of primary amines with diacrylates (at a 1 : 1.2 M ratio of amine : diacrylate). Finally, pBAE was obtained by end-capping modification of the resulting acrylate-terminated polymer with 3 arginine molecules at each end – H-Cys-Arg-Arg-Arg-NH_2 – named C6-CR3. The final molecular weight was approximately 3480 g mol^{-1}. The polymer was later labelled with Cy5 at a 1 dye per pBAE molecule ratio.

Poly(β-amino ester) polymer labelling

To label the polymers with cyanine 5 (Cy5), the following protocol was used. First, a solution of Cy5 NHS ester in DMSO (10 mg mL^{-1}) was prepared. In parallel, a solution of C6-CR3 (0.035 mL, 100 mg mL^{-1}, 0.97 μmol) in DMSO was prepared in a screw cap tube. An excess of triethylamine was added to the polymer solution, and following that, the Cy5 solution was poured inside. The solution was stirred in a dark environment, at 25 °C, for 20 h. Then, a mixture of 7/3 diethyl ether/acetone was added dropwise. The sample was centrifuged at 4000 rpm for 10 min to remove the solvent. This step was repeated twice.

Finally, the product was dried under vacuum and dissolved in 100 mg mL^{-1} DMSO.

Polyplex formulation

Polyplexes were prepared as detailed before.[26] In brief, they were formulated by mixing equal volumes of pGFP and pBAE polymer at a 1 : 25 weight ratio (w/w) in NaOAc buffer solution (12.5 mM, pH 5.0). pGFP was added over the polymer solution, mixed vigorously by pipetting, and the mixture was incubated for 30 minutes at 25 °C. Then, the mixture was added into an equal volume of Milli-Q H_2O, followed by another equal volume of HEPES buffer (20 Mm, pH 7.4) with 4 wt% of sucrose. Polyplexes were lyophilized and stored at −20 °C. On the day of use, they were redispersed in the initial preparation volume of Milli-Q water.

For optimal *d*STORM imaging, polyplexes were prepared using 1% Cy5 labelled pBAE and 25% Cy3 labelled pDNA. For nuclear entry studies, polyplexes were prepared with all pDNA molecules labelled.

DLS measurements

Hydrodynamic diameter (nm) and polydispersity index (PDI) measurements were performed with non-labelled polyplexes using a Zetasizer Nano-ZS (Malvern Instruments Ltd, Malvern, UK) at 25 °C and 633 nm laser wavelength and using a 173° signal detector. Three measurements of each nanoparticle batch were performed with 20 runs per measurement, taking into account the intensity approximation. Results correspond to the mean ± standard deviation of at least three independent nanoparticle batches.

FRET measurements

FRET measurements were carried out using a Tecan Infinite M200 Pro microplate reader. Each sample had a final volume of 50 μL and experiments were run in triplicate (mean and standard deviation are plotted). The FRET ratio is calculated by dividing the intensities at 570 nm and 670 nm, corresponding to the Cy3 and Cy5 emission maxima, respectively. To assess the dynamic behaviour of polyplexes, equal volumes of pBAE-Cy5 and pDNA-Cy3 labelled polyplexes were mixed just before the measurement. As a negative control, the two polyplex batches were measured independently without mixing. And as a positive control, polyplexes were prepared already with the two components labelled.

Polyplex sample preparation for dSTORM of free polyplexes

The microscopy slide consisted of a cover slip (24 mm × 24 mm, thickness 0.15 mm) attached to a glass slide with double-sided tape. Approximately, 35 μL of freshly resuspended polyplexes diluted 1/100 in PBS was added in the flow chamber. After 10 minutes of incubation at room temperature, unbound polyplexes were removed by washing excess sample with PBS. Finally, *d*STORM buffer (5% w/v glucose, 100 mM cysteamine, 0.5 mg mL^{-1} glucose oxidase and 40 μg mL^{-1} catalase in PBS) was fluxed into the chamber before imaging.

In vitro sample preparation

COS-7 cells (ATCC® CRL-1651™) were cultured in DMEM containing 10% FBS, 2 mM L-glutamine, 100 units per mL penicillin and 100 μg mL^{-1} streptomycin. Cells were seeded at a density of 30 000 cells per well with 400 μL of media in an 8-well Nunc™ Lab-Tek™ (Thermo Fisher Scientific®) and were allowed to grow overnight at 37 °C and 5% CO_2, to reach 70–90% confluence.

Cells were incubated with 400 μL of diluted polyplexes at a concentration of 3.75 ng pGFP μL^{-1} in full media. For trafficking studies, cells were incubated for 30 minutes in a standard CO_2 incubator, washed with PBS and grown for 0 h, 0.5 h, 2 h, 12 h, 24 h and 48 h before fixation. To study nuclear entry, cells were incubated with polyplexes for 48 h. The fixation procedure involved 15 minutes of incubation with 200 μL of 4% PFA at room temperature under stirring conditions. Then, the cells were washed 3 times with PBS and stored at 4 °C in the dark. For imaging purposes, 200 μL of *d*STORM buffer was added to each well.

Image acquisition

Images were acquired using NIS-Elements software in a Nikon Eclipse Ti microscope (Nikon Europe, Amsterdam). Cy5-labelled pBAE was imaged with a 647 nm laser (160 mW), Cy3-labelled pDNA was imaged with a 561 nm laser (80 mV) and GFP was imaged with a 488 nm laser (1.6 mW). The sample was illuminated using a total internal reflection fluorescence (TIRF) alignment system and the *z*-level was kept constant using a Nikon perfect focus system. Fluorescence was recorded using a Nikon 100×, 1.49 NA oil immersion objective and passed through a quad-band pass dichroic filter (97335 Nikon). Images were acquired onto a 256 × 256 pixel region (pixel size 0.16 μm) of a Hamamatsu 19 ORCA-Flash 4.0 camera at 10 and 50 ms integration time for *d*STORM and GFP imaging, respectively. For *d*STORM images, 21 000 and 20 000 frames were obtained for the 647 nm and the 567 nm channels, respectively. The 647 nm channel was obtained first, and the initial 1.000 frames were discarded.

Image and data analysis

To reconstruct *d*STORM images, single molecules in each frame were identified by fitting a 2D Gaussian function on the NIS Elements software from Nikon. The identification threshold (the difference between the number of photons collected in the peak pixels and the background pixels) is set to 250 for both channels. To avoid different molecules blinking consecutively, the trace length parameter is set from 1 to 5. This means that molecules identified in consecutive frames would be counted as one if it lasts for a maximum of five frames, or they would be discarded if it is more than 5 frames. Identified molecules were not filtered for the number of photons.

To objectively identify and quantify polyplexes, the list of localizations of the *d*STORM images were exported and analysed in a Matlab script previously described by Feiner-Gracia

et al.[45] Briefly, the pDNA localizations were clustered using a mean shift algorithm with a bandwidth of 80 nm. An ellipse was fitted on the obtained clusters in order to filter out clusters with an aspect ratio higher than 5. Other filters are also applied: minimum 30 localizations per cluster, maximum 350 nm diameter for the longest axis and minimum 300 nm distance between the cluster density centers. As an output, we obtained the number of localizations in each pDNA cluster and the pBAE localizations within 3 times the cluster radius.

In order to count the number of pDNA molecules in the nucleus, the same script was used; however, pBAE molecules were not quantified and clusters outside the nucleus were discarded. For this experiment, 50 images were analysed. Three outliers were discarded using *Cook's Distance* in the R software.

Conflicts of interest

There are no conflicts to declare.

Acknowledgements

The authors thanks the Spanish Ministry of Economy, Industry and Competitiveness, through Project SAF2016-75241-R, as part of the Generalitat de Catalunya through the CERCA program. L. A. thanks the European Research Council (ERC-StG- 757397).

References

1 Gene Therapy Clinical Trials Worldwide, http://www.abedia.com/wiley/indications.php (accessed January 2019).
2 W. W. Zhang, *et al.*, The First Approved Gene Therapy Product for Cancer Ad- p53 (Gendicine): 12 Years in the Clinic, *Hum. Gene Ther.*, 2018, **29**, 160–179.
3 M. Liang, Oncorine, the World First Oncolytic Virus Medicine and its Update in China, *Curr. Cancer Drug Targets*, 2018, **18**, 171–176.
4 N. Miller, Glybera and the future of gene therapy in the European Union, *Nat. Rev. Drug Discovery*, 2012, **11**, 419–419.
5 H. Ameri, Prospect of retinal gene therapy following commercialization of voretigene neparvovec-rzyl for retinal dystrophy mediated by RPE65 mutation, *J. Curr. Ophthalmol.*, 2018, **30**, 1–2.
6 X. Song, *et al.*, Targeted delivery of doxorubicin to breast cancer cells by aptamer functionalized DOTAP/DOPE liposomes, *Oncol. Rep.*, 2015, **34**, 1953–1960.
7 B. K. Kim, *et al.*, DOTAP/DOPE ratio and cell type determine transfection efficiency with DOTAP-liposomes, *Biochim. Biophys. Acta, Biomembr.*, 2015, **1848**, 1996–2001.
8 J. Lee and H. J. Ahn, PEGylated DC-Chol/DOPE cationic liposomes containing KSP siRNA as a systemic siRNA delivery Carrier for ovarian cancer therapy, *Biochem. Biophys. Res. Commun.*, 2018, **503**, 1716–1722.
9 C. Xu, H. Tian and X. Chen, Recent progress in cationic polymeric gene carriers for cancer therapy, *Sci. China: Chem.*, 2017, **60**, 319–328.
10 B. Shi, *et al.*, Challenges in DNA Delivery and Recent Advances in Multifunctional Polymeric DNA Delivery Systems, *Biomacromolecules*, 2017, **18**, 2231–2246.
11 G. R. Dhanya, D. S. Caroline, M. R. Rekha and K. Sreenivasan, Histidine and arginine conjugated starch-PEI and its corresponding gold nanoparticles for gene delivery, *Int. J. Biol. Macromol.*, 2018, **120**, 999–1008.
12 B. Xu, *et al.*, PEGylated dendrimer-entrapped gold nanoparticles with low immunogenicity for targeted gene delivery, *RSC Adv.*, 2018, **8**, 1265–1273.
13 B. Du, *et al.*, Lipid-Coated Gold Nanoparticles Functionalized by Folic Acid as Gene Vectors for Targeted Gene Delivery in vitro and in vivo, *ChemMedChem*, 2017, **12**, 1768–1775.
14 S. M. Hoy, Patisiran: First Global Approval, *Drugs*, 2018, **78**, 1625–1631.
15 U. Lächelt and E. Wagner, Nucleic Acid Therapeutics Using Polyplexes: A Journey of 50 Years (and Beyond), *Chem. Rev.*, 2015, **115**, 11043–11078.
16 J. Vangindertael, *et al.*, An introduction to optical super-resolution microscopy for the adventurous biologist, *Methods Appl. Fluoresc.*, 2018, **6**, 022003.
17 D. van der Zwaag, *et al.*, Super Resolution Imaging of Nanoparticles Cellular Uptake and Trafficking, *ACS Appl. Mater. Interfaces*, 2016, **8**, 6391–6399.
18 S. Pujals, N. Feiner-Gracia, P. Delcanale, I. Voets and L. Albertazzi, Super-resolution microscopy as a powerful tool to study complex synthetic materials, *Nat. Rev. Chem.*, 2019, **3**, 68–84.
19 M. Wojnilowicz, A. Glab, A. Bertucci, F. Caruso and F. Cavalieri, Super-resolution Imaging of Proton Sponge-Triggered Rupture of Endosomes and Cytosolic Release of Small Interfering RNA, *ACS Nano*, 2019, **13**, 187–202.
20 N. Feiner-Gracia, R. A. Olea, R. Fitzner, N. El Boujnouni, A. H. van Asbeck, R. Brock and L. Albertazzi, Super-resolution Imaging of Structure, Molecular Composition, and Stability of Single Oligonucleotide Polyplexes, *Nano Lett.*, 2019, **19**, 2784–2792.
21 M. J. Rust, M. Bates and X. Zhuang, Sub-diffraction-limit imaging by stochastic optical reconstruction microscopy (STORM), *Nat. Methods*, 2006, **3**, 793–796.
22 M. Heilemann, *et al.*, Subdiffraction-Resolution Fluorescence Imaging with Conventional Fluorescent Probes, *Angew. Chem., Int. Ed.*, 2008, **47**, 6172–6176.
23 P. R. Nicovich, D. M. Owen and K. Gaus, Turning single-molecule localization microscopy into a quantitative bioanalytical tool, *Nat. Protoc.*, 2017, **12**, 453–460.
24 J. J. Green, *et al.*, Biodegradable Polymeric Vectors for Gene Delivery to Human Endothelial Cells, *Bioconjugate Chem.*, 2006, **17**, 1162–1169.
25 J. J. Green, R. Langer and D. G. Anderson, A Combinatorial Polymer Library Approach Yields Insight into Nonviral Gene Delivery, *Acc. Chem. Res.*, 2008, **41**, 749–759.

26 N. Segovia, P. Dosta, A. Cascante, V. Ramos and S. Borrós, Oligopeptide-terminated poly(β-amino ester)s for highly efficient gene delivery and intracellular localization, *Acta Biomater.*, 2014, **10**, 2147–2158.

27 J. C. Sunshine, M. I. Akanda, D. Li, K. L. Kozielski and J. J. Green, Effects of Base Polymer Hydrophobicity and End-Group Modification on Polymeric Gene Delivery, *Biomacromolecules*, 2011, **12**, 3592–3600.

28 T. T. Smith, *et al.*, In situ programming of leukaemia-specific T cells using synthetic DNA nanocarriers, *Nat. Nanotechnol.*, 2017, **12**, 813–820.

29 F. Yang, *et al.*, Genetic engineering of human stem cells for enhanced angiogenesis using biodegradable polymeric nanoparticles, *Proc. Natl. Acad. Sci. U. S. A.*, 2010, **107**, 3317–3322.

30 H. Devalapally, D. Shenoy, S. Little, R. Langer and M. Amiji, Poly(ethylene oxide)-modified poly(beta-amino ester) nanoparticles as a pH-sensitive system for tumor-targeted delivery of hydrophobic drugs: part 3. Therapeutic efficacy and safety studies in ovarian cancer xenograft model, *Cancer Chemother. Pharmacol.*, 2007, **59**, 477–484.

31 S. Y. Tzeng, *et al.*, Non-viral gene delivery nanoparticles based on Poly(β-amino esters) for treatment of glioblastoma, *Biomaterials*, 2011, **32**, 5402–5410.

32 P. Dosta, N. Segovia, A. Cascante, V. Ramos and S. Borrós, Surface charge tunability as a powerful strategy to control electrostatic interaction for high efficiency silencing, using tailored oligopeptide-modified poly(beta-amino ester)s (PBAEs), *Acta Biomater.*, 2015, **20**, 82–93.

33 P. Dosta Pons, *Development of cell-specific RNAi delivery vectors based on poly(β-amino ester)s with therapeutic applications*, Universitat Ramon Llull, 2017.

34 P. Dosta, V. Ramos and S. Borrós, Stable and efficient generation of poly(β-amino ester)s for RNAi delivery, *Mol. Syst. Des. Eng.*, 2018, **3**, 677–689.

35 C. Fornaguera, *et al.*, mRNA Delivery System for Targeting Antigen-Presenting Cells In Vivo, *Adv. Healthcare Mater.*, 2018, **7**, 1800335.

36 C. Troiber, *et al.*, Comparison of four different particle sizing methods for siRNA polyplex characterization, *Eur. J. Pharm. Biopharm.*, 2013, **84**, 255–264.

37 P. Dosta, N. Segovia, A. Cascante, V. Ramos and S. Borrós, Surface charge tunability as a powerful strategy to control electrostatic interaction for high efficiency silencing, using tailored oligopeptide-modified poly(beta-amino ester)s (PBAEs), *Acta Biomater.*, 2015, **20**, 82–93.

38 S. Vaidyanathan, J. Chen, B. G. Orr and M. M. Banaszak Holl, Cationic Polymer Intercalation into the Lipid Membrane Enables Intact Polyplex DNA Escape from Endosomes for Gene Delivery, *Mol. Pharm.*, 2016, **13**, 1967–1978.

39 J. Chen, *et al.*, Cationic Nanoparticles Induce Nanoscale Disruption in Living Cell Plasma Membranes, *J. Phys. Chem. B*, 2009, **113**, 11179–11185.

40 S. Vaidyanathan, *et al.*, Quantitative Measurement of Cationic Polymer Vector and Polymer–pDNA Polyplex Intercalation into the Cell Plasma Membrane, *ACS Nano*, 2015, **9**, 6097–6109.

41 M. J. Reilly, J. D. Larsen and M. O. Sullivan, Polyplexes Traffic through Caveolae to the Golgi and Endoplasmic Reticulum en Route to the Nucleus, *Mol. Pharm.*, 2012, **9**, 1280–1290.

42 K. M. Fichter, N. P. Ingle, P. M. McLendon and T. M. Reineke, Polymeric Nucleic Acid Vehicles Exploit Active Inter-Organelle Trafficking Mechanisms, *ACS Nano*, 2013, **7**, 347–364.

43 N. L. Ross and M. O. Sullivan, Importin-4 Regulates Gene Delivery by Enhancing Nuclear Retention and Chromatin Deposition by Polyplexes, *Mol. Pharm.*, 2015, **12**, 4488–4497.

44 J. D. Larsen, N. L. Ross and M. O. Sullivan, Requirements for the nuclear entry of polyplexes and nanoparticles during mitosis: Nuclear entry during mitosis, *J. Gene Med.*, 2012, **14**, 580–589.

45 N. Feiner-Gracia, M. Beck, S. Pujals, S. Tosi, T. Mandal, C. Buske, M. Linden and L. Albertazzi, Super- Resolution Microscopy Unveils Dynamic Heterogeneities in Nanoparticle Protein Corona, *Small*, 2017, **13**, 1701631.